

TRANSFUSION MEDICINE

Rapid clearance of storage-induced microerythrocytes alters transfusion recovery

Camille Roussel,^{1,4,*} Alexandre Morel,^{1,2,5,*} Michaël Dussiot,^{1,2,*} Mickaël Marin,^{2,4} Martin Colard,^{1,2} Aurélie Fricot-Monsinjon,^{2,4} Anaïs Martinez,^{1,2} Charlotte Chambrion,^{2,4} Benoît Henry,^{2,4} Madeleine Casimir,^{1,2} Geoffroy Volle,^{2,4} Mallorie Dépond,^{2,4} Safi Dokmak,⁶ François Paye,⁷ Alain Sauvanet,⁶ Caroline Le Van Kim,^{2,4} Yves Colin,^{2,4} Sonia Georgeault,⁸ Philippe Roingard,^{8,9} Steven L. Spitalnik,¹⁰ Papa Alioune Ndour,^{2,4} Olivier Hermine,^{1,2,5} Eldad A. Hod,¹⁰ Pierre A. Buffet,^{2,4,11,†} and Pascal Amireault^{1,4,†}

¹U1163, Laboratory of Cellular and Molecular Mechanisms of Hematological Disorders and Therapeutic Implications, INSERM, Université de Paris, Paris, France; ²Laboratoire d'Excellence GR-Ex, Paris, France; ³UMR_S1134, Biologie Intégrée du Globule Rouge, INSERM, Université de Paris, Paris, France; ⁴Institut National de la Transfusion Sanguine, Paris, France; ⁵Département d'Hématologie, Hôpital Universitaire Necker Enfants Malades, Assistance Publique-Hôpitaux de Paris (AP-HP), Paris, France; ⁶Department of Hepatobiliary Surgery and Liver Transplantation, Hôpital Beaujon, AP-HP, Clichy, France; ⁷Department of Digestive Surgery, Hôpital Saint-Antoine, AP-HP, Paris, France; ⁸Plateforme des Microscopies, Infrastructures de Recherche en Biologie Santé et Agronomie, Programme Pluri-Formation Analyse des Systèmes Biologiques and ⁹U1259, Morphogenèse et Antigénicité du VIH et des Virus des Hépatites, INSERM, Université de Tours and Centre Hospitalier Régional Universitaire (CHRU) de Tours, Tours, France; ¹⁰Department of Pathology and Cell Biology, Irving Medical Center, Columbia University, New York, NY; and ¹¹AP-HP, Paris, France

KEY POINTS

- When SMEs are abundant in RBC concentrates, transfusion recovery is diminished.
- SMEs are rapidly cleared after transfusion predominantly through spleen- and macrophage-related mechanisms.

Permanent availability of red blood cells (RBCs) for transfusion depends on refrigerated storage, during which morphologically altered RBCs accumulate. Among these, a subpopulation of small RBCs, comprising type III echinocytes, spherocytes, and spherocytes and defined as storage-induced microerythrocytes (SMEs), could be rapidly cleared from circulation posttransfusion. We quantified the proportion of SMEs in RBC concentrates from healthy human volunteers and assessed correlation with transfusion recovery, investigated the fate of SMEs upon perfusion through human spleen ex vivo, and explored where and how SMEs are cleared in a mouse model of blood storage and transfusion. In healthy human volunteers, high proportion of SMEs in long-stored RBC concentrates correlated with poor transfusion recovery. When perfused through human spleen, 15% and 61% of long-stored RBCs and SMEs were cleared in 70 minutes, respectively. High initial proportion of SMEs also correlated with high retention of RBCs by perfused human spleen. In the mouse model, SMEs accumulated during storage. Transfusion of long-stored RBCs resulted in reduced posttransfusion recovery, mostly due to SME clearance. After transfusion in mice, long-stored RBCs accumulated predominantly in spleen and were ingested mainly by splenic and hepatic macrophages. In macrophage-depleted mice, splenic accumulation and SME clearance were delayed, and transfusion recovery was improved. In healthy hosts, SMEs were cleared predominantly by macrophages in spleen and liver. When this well-demarcated subpopulation of altered RBCs was abundant in RBC concentrates, transfusion recovery was diminished. SME quantification has the potential to improve blood product quality assessment. This trial was registered at www.clinicaltrials.gov as #NCT02889133. (*Blood*. 2021;137(17):2285-2298)

Introduction

Maintaining the permanent availability of human red blood cells (RBCs) for transfusion depends on refrigerated storage of RBC concentrates for up to 42 days. The potential impact of storage duration on transfusion safety has been extensively studied.¹⁻⁵ Meta-analyses of prospective randomized controlled trials suggest there is no advantage in terms of mortality in transfusing short-stored, as compared with standard-issue, RBC concentrates.^{6,7} A secondary analysis of the INFORM trial⁸ concluded that RBCs stored for >35 days were not associated with an increased mortality risk; however, no randomized trials

have addressed whether the oldest blood is associated with harm. Therefore, questions remain regarding the clinical impact of long-stored RBC concentrates in general and on massive transfusion in particular, with few studies and discordant results,^{9,10} or in chronically transfused patients, who are susceptible to transfusion-related iron overload.

The term storage lesions refers to the alterations that accumulate during hypothermic storage.¹¹⁻¹⁶ The intensity of storage lesions varies from donor to donor,¹⁷⁻²⁰ and despite extensive studies in vitro,^{14,21,22} its impact on transfusion outcome remains unclear.

The wealth of analyses on RBC transfusion safety sharply contrasts with the small number of studies evaluating the impact of storage duration on transfusion recovery. For example, a study of autologous transfusion of ^{51}Cr -labeled RBCs in healthy volunteers showed that storage duration was associated with decreased posttransfusion recovery and increased extravascular hemolysis, serum transferrin saturation, and circulating non-transferrin-bound iron.²³ In addition, in retrospective studies, transfusion-induced hemoglobin increments were significantly decreased when RBC concentrates were stored for longer durations.²⁴⁻²⁶ The 24-hour posttransfusion recovery was also significantly decreased when patients with hematological malignancies were transfused with irradiated RBC concentrates stored for >2 weeks compared with irradiated RBC concentrates stored for <2 weeks.¹⁷ These studies suggest that rapid clearance of long-stored RBCs results in reduced transfusion recovery. Early studies showed that some *in vitro* markers of storage lesions, such as storage hemolysis, correlated poorly with transfusion recovery.²⁷ Although other *in vitro* markers, such as ATP level and the morphology index, have shown better correlation with transfusion recovery, the predictive value of these markers is limited.²⁸⁻³⁵ Finally, direct evidence is lacking that RBCs with low levels of ATP or morphologically altered RBCs are indeed the target for early posttransfusion clearance.

A well-demarcated subpopulation of morphologically altered and smaller RBCs, comprising type III echinocytes, spherocytocytes, and spherocytes, is easily quantified by imaging flow cytometry in a reproducible, objective, and operator-independent manner.³⁶ Their decreased surface area, resulting from progressive membrane loss during storage,³⁷⁻³⁹ is expected to lead to their rapid clearance from the recipient's circulation after transfusion. Indeed, the decreased surface area of chemically treated RBCs leads to splenic entrapment.⁴⁰ These small RBCs, defined as storage-induced microerythrocytes (SMEs), accumulate during storage, reaching a mean proportion of 24% of the entire RBC population at day 42 of storage.³⁶ Rapid clearance of this subpopulation could explain the decreased transfusion recovery observed after transfusion of long-stored RBC concentrates.

Herein, we assessed whether the proportion of SMEs in stored RBC concentrates correlates with posttransfusion recovery in healthy volunteers. We also investigated the fate of SMEs during *ex vivo* perfusion of human spleen, as well as in a specifically developed mouse model. Converging results obtained in human participants and mice confirmed that SMEs are rapidly cleared after transfusion, predominantly through spleen- and macrophage-related mechanisms.

Methods

RBC concentrate collection and storage

Leukoreduced RBC concentrates from healthy donors were stored in saline-adenine-glucose-mannitol (SAGM) solution at 2 to 6°C for 42 days and provided by the Etablissement Français du Sang Haut de France-Normandie (French blood banking system). Samples were aseptically collected for each experiment. For human ^{51}Cr RBC posttransfusion recovery studies, leukoreduced RBC concentrates in additive solution-3 (AS-3; $n = 30$) or AS-1 ($n = 1$) were collected from consented healthy

volunteers and stored at 2 to 6°C. On day 40 to 42 of storage, 20 to 30 mL were aseptically retrieved from the bag to perform ^{51}Cr labeling of RBCs and 24-hour posttransfusion recovery experiments as described.^{23,41,42} At the same time, a second aliquot of RBCs was immediately shipped at 4°C from Columbia University to Institut National de la Transfusion Sanguine for SME quantification (which occurred 40-48 hours after posttransfusion recovery study). Technical details on RBC concentrate collection are available in the supplemental Methods, available on the *Blood* Web site.

Scanning electron microscopy of human samples

Samples were fixed by incubation in 4% paraformaldehyde and 1% glutaraldehyde in 0.1 M of phosphate buffer (pH, 7.3), washed in phosphate buffer, and postfixed by incubation with 2% osmium tetroxide for 1 hour. Samples were then fully dehydrated in a graded series of ethanol solutions and dried in hexamethyldisilazane. Finally, samples were coated with 4 nm of carbon using a GATAN PECS 682 apparatus before observation under a Zeiss Ultra plus field emission gun scanning electron microscope.

Imaging flow cytometric analysis of human samples

Imaging flow cytometry using ImageStream X Mark II (Amnis of EMD Millipore) was performed to determine RBC dimensions and morphology by using brightfield images ($\times 60$ magnification) processed with computer software (IDEAS [version 6.2]; Amnis) as described.³⁶ Technical details are available in supplemental Methods.

Human spleen retrieval and *ex vivo* perfusion

Spleens were retrieved and processed as described.⁴³ All patients underwent distal splenopancreatectomy for pancreatic disease. Spleens were macroscopically and microscopically normal in all cases. Main splenic artery was cannulated, and spleens were flushed with cold Krebs-albumin solution for transport to the laboratory. Spleens were coperfused with untreated long-stored RBCs (stained with Celltrace Violet, CellTrace Yellow, or 8 $\mu\text{g}/\text{mL}$ of biotin), rejuvenated long-stored RBCs (stained with carboxyfluorescein diacetate succinimidyl ester [CFSE], Celltrace Far Red, or 32 $\mu\text{g}/\text{mL}$ of biotin), and short-stored RBCs, at a final hematocrit of 5% to 30% (Krebs-albumin solution), over a 70-minute period at 37°C. Samples were retrieved from the circuit for flow cytometric or imaging flow cytometric analysis. Persistence in circulation was calculated using the following formula: (% stained RBCs in sample/% stained RBCs at T0) \times 100. Mean retention rate was calculated using the following formula: $100 - ((\text{mean \% of stained RBCs in all samples taken between 40 and 70 minutes} / \text{\% of stained RBCs at T0}) \times 100)$. Rejuvenation was conducted by adding 3 mL of rejuvenation solution (Zimmer Biomet) to 20 mL of RBCs and incubating 1 hour at 37°C, followed by 2 washes in SAGM solution.

Mouse blood banking and transfusion

Intact, splenectomized, or sham splenectomized C57BL/6 female mice (age 8-10 weeks) were purchased from Janvier Laboratory. RBCs were aseptically collected in citrate-phosphate-dextrose-adenine solution, leukoreduced, and stored at 4°C for up to 14 days as previously reported.⁴⁴ For macrophage depletion, mice were intraperitoneally injected with 1 and 0.5 mg of clodronate liposomes (Liposoma) 5 and 2 days before

transfusion, respectively. RBCs were stained with CFSE (20 μ M) and washed twice in RPMI. CFSE⁺ RBC suspensions (200 μ L) were transfused through the retro-orbital plexus, and their proportion after transfusion was measured by flow cytometry. Posttransfusion recovery was calculated using the following formula: (% CFSE⁺ RBCs in sample/% CFSE⁺ RBCs in 5-minute sample) \times 100.

Imaging flow cytometric analysis of mouse samples

Blood bank or transfused mouse samples were diluted (1:100) in Dulbecco's phosphate-buffered saline (PBS) supplemented with 1 g/L of glucose and 0.01% bovine serum albumin (pH, 7.3), incubated for 50 minutes at 37°C, and analyzed by imaging flow cytometry as for human samples. Transfused RBCs were analyzed by gating on CFSE⁺ events. Posttransfusion recovery of the SME subpopulation was calculated using the following formula: posttransfusion recovery \times (% of CFSE⁺ RBCs <41 μ m² in sample/% of CFSE⁺ RBCs <41 μ m² in 5-minute sample).

Enrichment in organs

Spleen and liver were sliced in PBS, 2% fetal bovine serum, and 2 mM of EDTA, and bone marrow cells were obtained by flushing the bones. After 15-minute incubation at room temperature, supernatants were collected, filtered (40 μ m), and stained with the DNA stain Draq5. Samples were analyzed by flow cytometry, and the enrichment factor (EF) was calculated using the following formula: (% of CFSE⁺ RBCs within Draq5⁺ cells of organ/% of CFSE⁺ RBCs in blood sample) \times 100.

In vivo erythrophagocytosis

Spleen and liver cells were dissociated mechanically using dedicated dissociation kits and gentleMACS dissociator (Miltenyi Biotec). Bone marrow cells were obtained by flushing tibia and femur with PBS, 2% fetal bovine serum, and 2 mM of EDTA. RBCs were removed from the suspension using ACK lysing buffer (Invitrogen). Cells were first incubated with anti-mouse CD16/CD32 clone 2.4G2 to block immunoglobulin G receptors (BD). Cells were then stained at 4°C using a panel of antibodies and analyzed by flow cytometry (supplemental Methods).

Statistics

Calculations for statistical differences between various groups were carried out using the analysis of variance technique and the Sidak, Tukey, or Kruskal-Wallis posttest to correct for multiple comparisons, as indicated in the figure legends. The Spearman test was used to assess correlation between SMEs and posttransfusion recovery in human volunteers and in ex vivo perfusion of human spleen. Otherwise, the 2-tailed paired Student *t* test was used. A *P* value <.05 was considered statistically significant. Statistical analyses were performed using Prism software (GraphPad).

Study approval

The study was conducted according to the Declaration of Helsinki, and all research participants provided written informed consent before study participation. The study was approved by the Columbia University Irving Medical Center and Institutional Review Board (#00001072). Human spleens were retrieved in the context of the Splenvivo project approved by the "Ile-de-France II" Institutional Review Board on 4 September 2017 (#CPP 2015-02-05 SM2 DC). Animal experiments were

conducted according to European Directives and were approved by the French Ministry of Education and Research (#12071-2017012712012626 v5).

Results

Accumulation of morphologically altered RBCs during storage

At the beginning of storage, scanning electron microscopic images showed that discocytes were abundant, and only a few morphologically altered RBCs could be observed (Figure 1Ai-ii). By 41 days of storage, morphologically altered RBCs were abundant, and fewer discocytes were observed (Figure 1Aiii-iv). RBC shapes, presented according to the Bessis classification,⁴⁵ included discocytes, type I, II, and III echinocytes, spherocytocytes, and spherocytes (Figure 1B); the last 3 categories composed the SME subpopulation.³⁶ These qualitative observations confirm the evolution of RBC morphology during storage.^{22,30,46-48}

Proportions of SMEs at the end of storage display high interdonor variability

We quantified SMEs weekly throughout storage in 24 RBC concentrates collected from healthy human donors and stored in SAGM solution. For all donors, mean SMEs (range \pm standard deviation [SD]) accumulation during storage ranged from 5.2% (1.1%-9.8% \pm 2.4%) on day 3 to 24.6% (4.9%-68.1% \pm 13.6%) on day 42, with marked interdonor variability (Figure 2A). We defined low- and high-SME RBC concentrates by cutoff proportions of SMEs < -1 SD and > +1 SD at the end of storage, respectively. Low- and high-SME concentrates accounted for 12.5% and 21% of RBC concentrates, respectively. These proportions of SMEs are broadly similar to the proportions of RBCs cleared in human posttransfusion recovery studies.²⁰

High proportions of SMEs in long-stored RBC concentrates correlate with poor transfusion recovery in healthy human volunteers

We examined correlation of pretransfusion proportions of SMEs in autologous RBC concentrates (stored in AS-3 or AS-1 for 42 days) with 24-hour posttransfusion recovery (using ⁵¹Chr-labeling procedure⁴¹) in 31 healthy volunteers. As observed with RBCs stored in SAGM solution, the projected surface area on normalized frequency plots displayed a bimodal distribution for all donors, enabling quantification of SMEs in each RBC concentrate (Figure 2B). Mean percentage of SMEs was 19.9%, and variability among volunteers was similarly wide, with extreme values of 6% and 52% (Figure 2C). Mean (range \pm SD) 24-hour posttransfusion recovery was 83.5% (71.5%-95.5% \pm 4.8%). One of the 31 volunteers had 24-hour posttransfusion recovery of 71.5%, which was below the US Food and Drug Administration guideline of 75%. The proportion of pretransfusion SMEs negatively correlated with 24-hour posttransfusion recovery (*P* = .02; Spearman *r* = -0.42; *r*² = 0.24; Figure 2C). Mean posttransfusion recovery was significantly decreased (*P* = .03) in high-SME RBC concentrates (78%) when compared with low-SME RBC concentrates (85%).

Most SMEs are rapidly cleared upon ex vivo perfusion of human spleen

We quantified the persistence of long-stored RBCs (14 RBC concentrates stored for 35-42 days in SAGM solution) mixed with

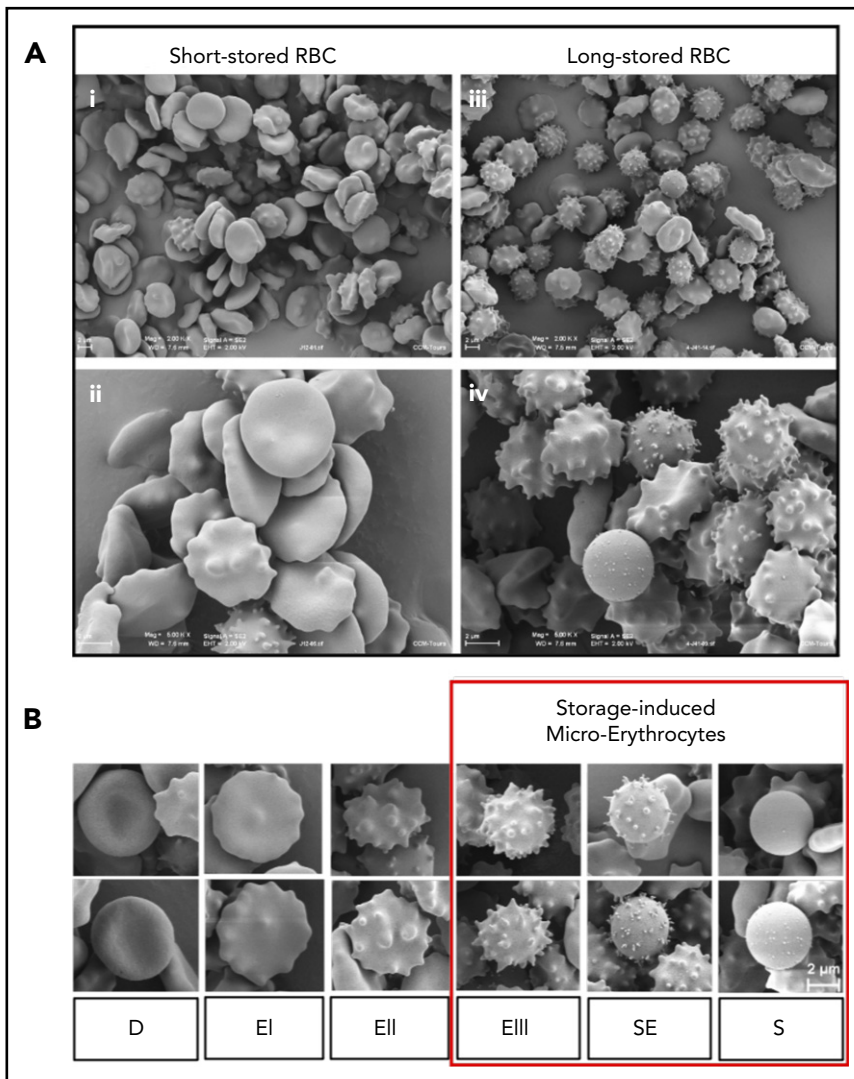


Figure 1. Accumulation of morphologically altered RBCs during storage. (A) Panoramic ($\times 2000$) (i) and detailed ($\times 5000$) (ii) views of short-stored RBC sample (day 12 of storage) containing a majority of discocytes (D) and type I (EI) or II echinocytes (EII), and panoramic ($\times 2000$) (iii) and detailed ($\times 5000$) (iv) views of long-stored RBC sample (day 41 of storage) containing abundant EIII, spherocytocytes (SE), and spherocytes (S). (B) Representative scanning electron images of RBC shapes observed during storage in SAGM: D, EI, EII, EIII, SE, and S; numerically zoomed regions from $2000\times$ acquisitions. Red square highlights morphologically altered RBCs defined as SMEs. Scale bars = $2\ \mu\text{M}$.

short-stored RBCs (stored for 3-12 days) in circulation during ex vivo perfusion of human spleen. The morphology of RBCs was similar in the perfusion medium and fresh plasma (supplemental Figure 1). RBCs were or were not rejuvenated using a procedure that improves intracellular ATP levels.⁴⁹ Mean proportion of long-stored RBCs in circulation decreased by 14.6% ($P < .01$) in 70 minutes, with marked interdonor variability (Figure 3A). Rejuvenation restored the projected surface area of RBCs to a normal Gaussian distribution by imaging flow cytometry (similar to that observed at beginning of storage), decreased the proportion of SMEs (Figure 3B), and induced improvement in the circulatory lifespan that reached statistical significance at 1, 1.5, 2, 5, and 40 minutes of perfusion ($P = .01, .003, .009, .03, \text{ and } .02$, respectively). The proportion of SMEs was also quantified during ex vivo perfusion. Projected surface area showed a bimodal distribution before perfusion and rapid clearance of SMEs (Figure 3C). The proportion of SMEs decreased during perfusion from a mean (range) of 20.0% (3.3%-36.1%) initially to 7.8% (2.2%-16.2%) at the end ($P = .02$; Figure 3D). The initial proportion of SMEs in untreated or rejuvenated RBC concentrates correlated with the mean retention rate in human spleen ($P = .03$; Spearman $r = 0.5$; Figure 3E). In contrast, in vitro storage hemolysis, intracellular

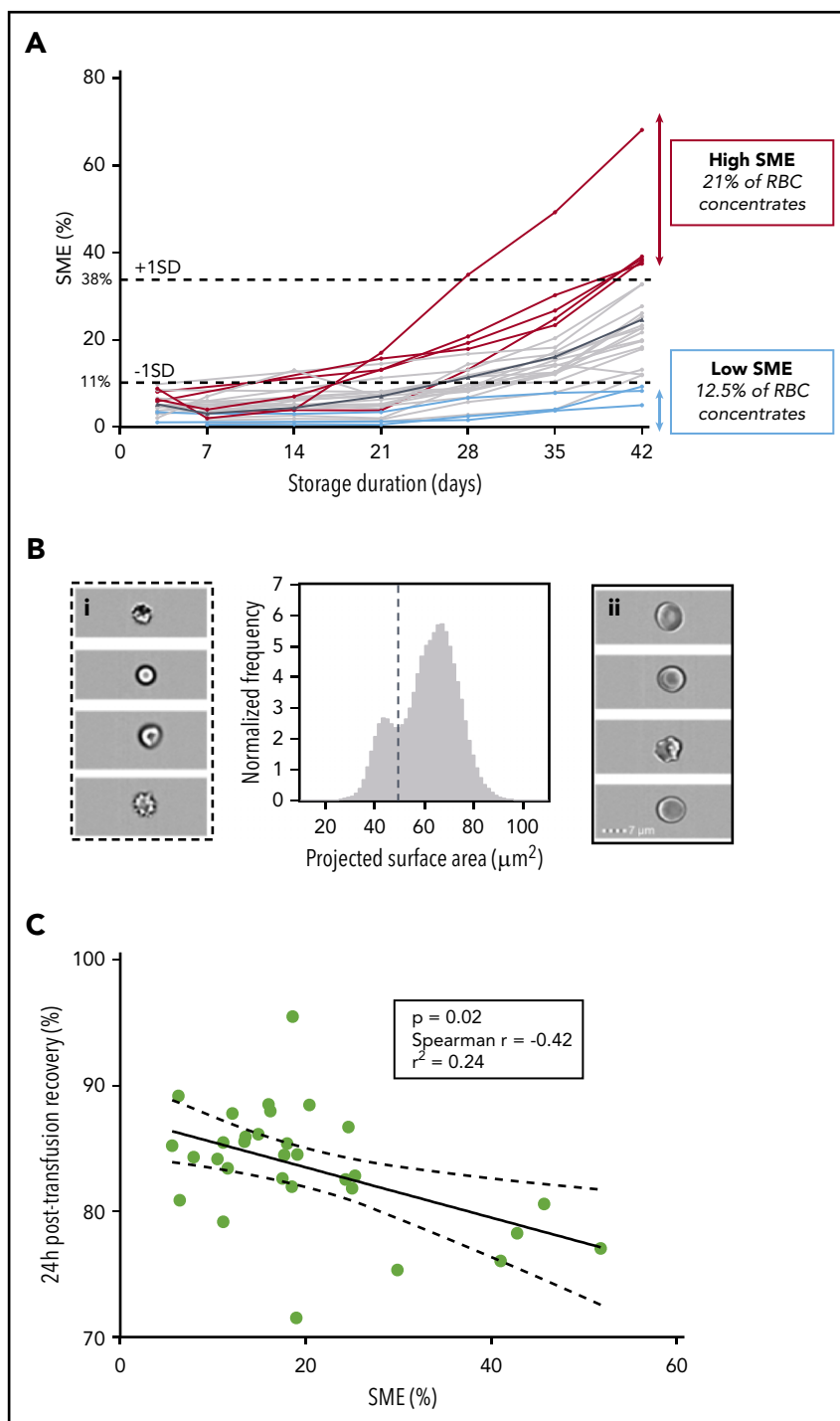
ATP level, and deformability did not correlate with retention rate (supplemental Figure 2).

SMEs accumulate during storage in mouse model of RBC storage

We developed a mouse model of RBC storage and transfusion to assess the fate of SMEs in vivo and determine the main mechanisms of RBC clearance. Long-stored RBCs showed lower 24-hour posttransfusion recovery rate ($61.9\% \pm 2.4\%$) compared with short-stored RBCs ($94.7\% \pm 0.9\%$; $P < .001$; Figure 4A).

Morphological alterations of stored mouse RBCs were quantified by adapting the imaging flow cytometric approach previously applied to human RBCs. Projected surface area showed a Gaussian distribution for short-stored and fresh RBCs, the latter collected immediately before analysis (Figure 4B). The distribution of long-stored RBCs was shifted to the left, indicating that some RBCs lost projected surface area (Figure 4C). Mean projected surface area was 47.0 and $47.1\ \mu\text{m}^2$ for fresh and short-stored RBCs, respectively; in contrast, it was significantly reduced to $43.0\ \mu\text{m}^2$ for long-stored RBCs ($P < .0001$; Figure 4D). Morphological analysis of imaging flow cytometric

Figure 2. Proportion of SMEs at the end of storage correlates with 24-hour posttransfusion recovery in healthy human volunteers. (A) Quantification of SMEs upon storage of RBC concentrates in SAGM solution ($n = 24$) between days 3 and 42 (mean value in solid black line). Low (blue lines) and high proportions of SMEs (red lines) defined by proportions of SME < -1 SD (11%) and $> +1$ SD (38%) at the end of storage, respectively. (B) Representative normalized frequency plot for RBC concentrate at the end of storage in AS-3 showing a well-demarcated subpopulation of SMEs. Subpopulation of SMEs contains spherocytes, spherocytocytes, and type III echinocytes (i), whereas normal-sized RBCs (ii) contain discocytes and type I and II echinocytes. (C) Correlation between 24-hour posttransfusion recovery and proportions of SMEs quantified by imaging flow cytometry at the end of storage ($n = 31$; $P = .02$; Spearman $r = -0.42$; $r^2 = 0.24$).



brightfield images categorized long-stored RBCs into either altered RBCs (type III echinocytes, spherocytocytes, spherostomatocytes, and spherocytes) or normal RBCs (type I and II echinocytes, stomatocytes, and discocytes). As shown in Figure 4E, altered RBCs had a mean projected area of $36.5 \mu\text{m}^2$ and corresponded to RBCs with a lower projected area, whereas RBCs categorized as normal had a profile similar to that of short-stored RBCs. In contrast to stored human RBCs, which showed a bimodal distribution, the 2 subpopulations of mouse RBCs overlapped on the projected area distribution profile in mice. Receiver operating characteristic analysis

allowed determination of a gating threshold, set at $41 \mu\text{m}^2$, which enabled robust identification of altered RBCs (supplemental Figure 3). Using this threshold, the proportion of SMEs was 13.5% and 36.1% in short- and long-stored RBCs, respectively ($P < .001$; Figure 4F).

SMEs are rapidly cleared from circulation of transfused mice

Imaging flow cytometry was used to determine the fate of circulating long-stored RBCs posttransfusion. Transfused RBCs with reduced surface area were detected in circulation of

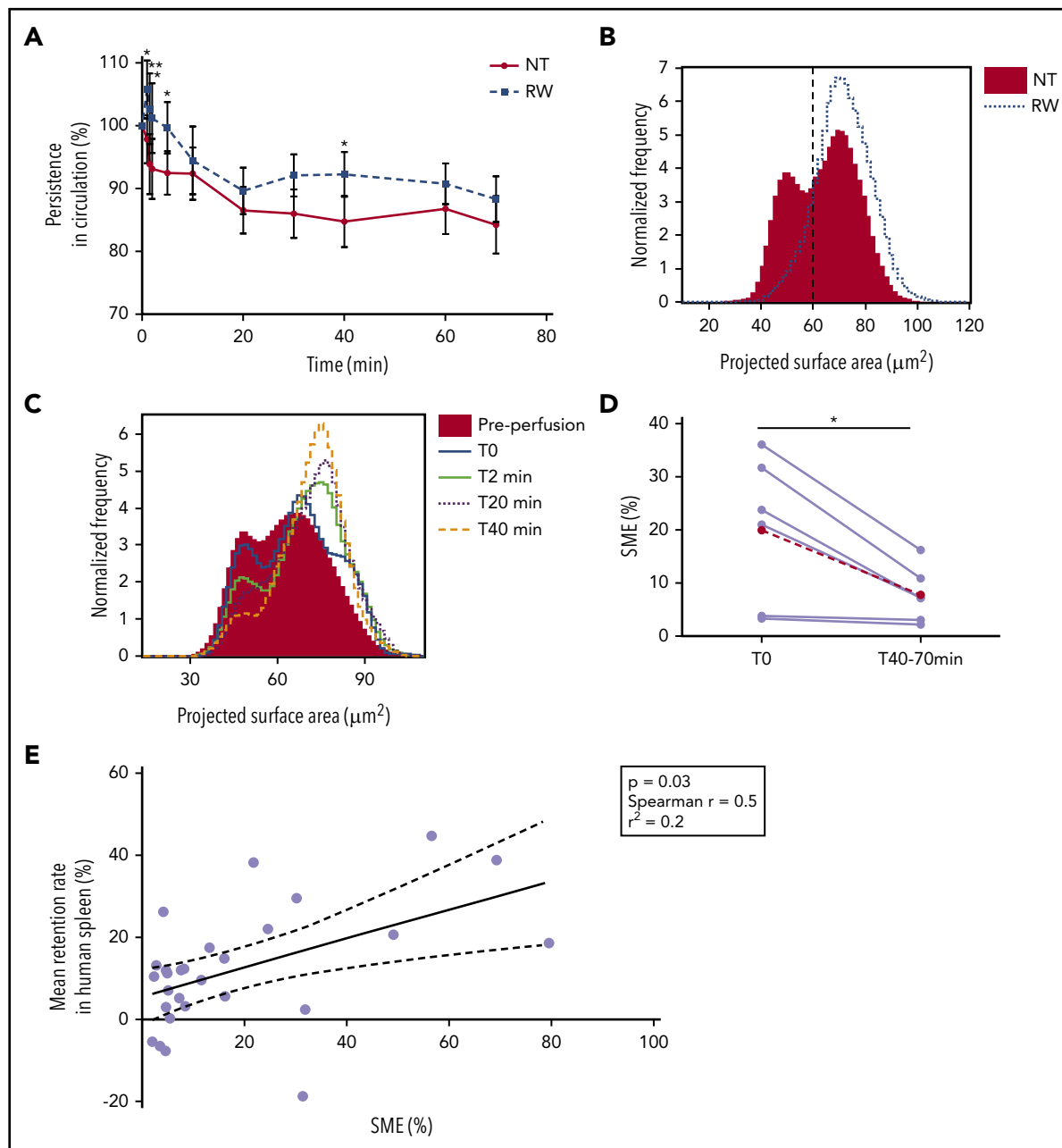
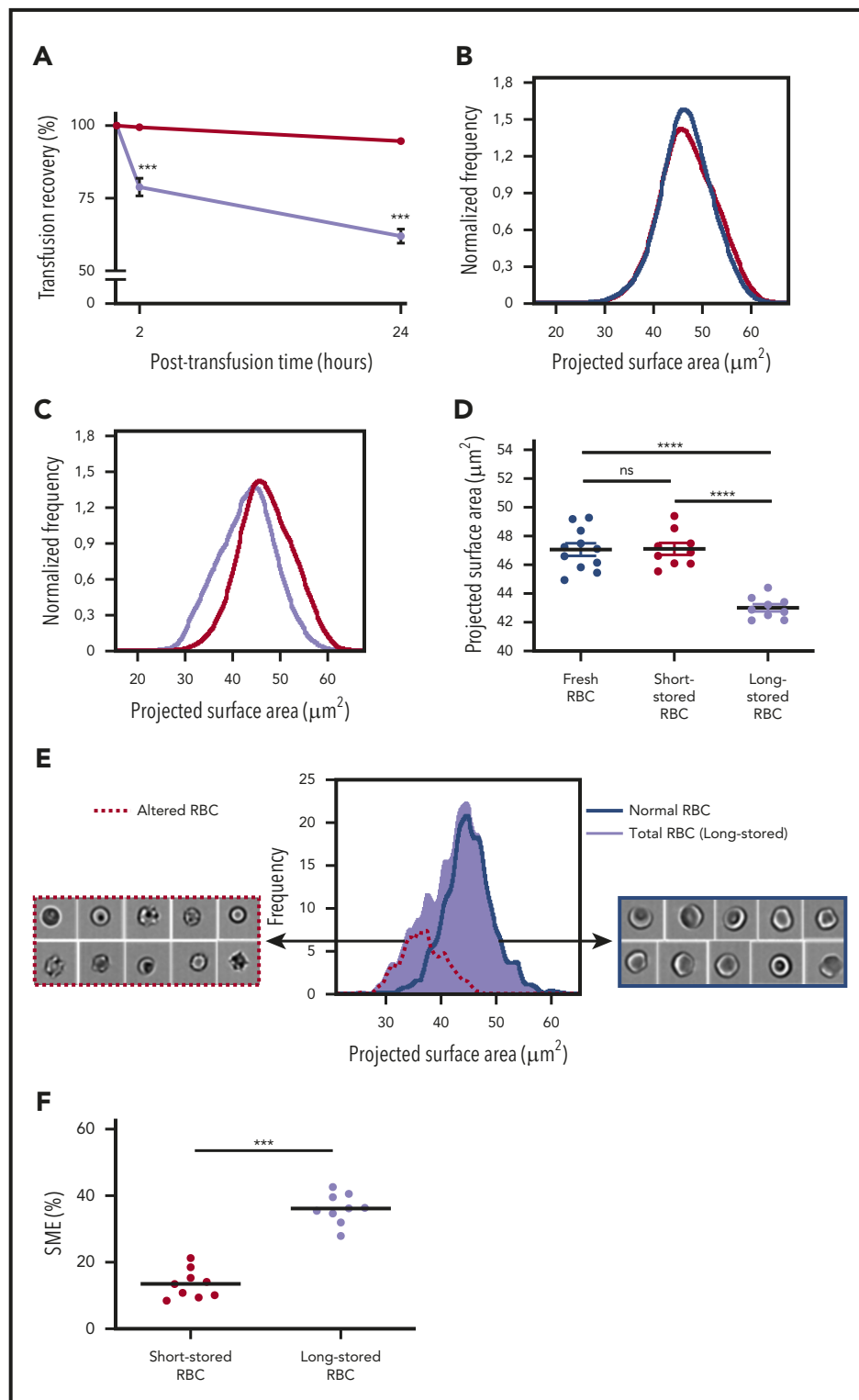


Figure 3. SMEs are rapidly cleared when perfused through human spleen ex vivo. (A) Kinetics (means \pm standard errors of the mean) of the normalized concentration in the perfusate of human spleen ex vivo ($n = 7$) of 14 RBC concentrates stored for 35 to 42 days and rejuvenated (RW; dashed line) or not (NT; solid line). (B) Representative normalized frequency plot of the projected surface area of RBCs stored for 42 days before (solid red histogram) and after (dotted line) rejuvenation. Dashed vertical line defines the gating cutoff for SMEs. (C) Representative frequency plot of projected surface area of stored RBCs (37 days) before (red histogram) and at different time points after perfusion through human spleen ex vivo (0 minutes, solid blue line; 2 minutes, solid green line; 20 minutes, dotted black line; and 40 minutes, dashed orange line). (D) Proportion of SMEs at the beginning (T0) and mean proportion of SMEs at all observations between 40 and 70 minutes (T40-70min) of perfusion through human spleen ex vivo ($n = 6$; red dashed line represents mean). (E) Correlation between mean retention rate in human spleen perfused ex vivo and proportion of SMEs in the RBC concentrate before transfusion ($n = 28$; $P = .03$; Spearman $r = 0.5$; $r^2 = 0.2$). $*P < .05$, $**P < .01$ by Sidak multiple comparisons test comparing, at each time point, the persistence in circulation of rejuvenated vs nontreated RBCs (A) or by paired Student t test comparing proportion of SMEs at T0 vs T40-70min (D).

recipients 5 minutes posttransfusion (Figure 5A). However, at 2 hours, an intermediate distribution profile was observed, and at 24 hours, the distribution profile of transfused RBCs was similar to that of fresh RBCs. SMEs were progressively cleared from circulation, declining from 30.5% at 5 minutes posttransfusion to 20.1% at 2 hours and 9.3% at 24 hours. When compared with the proportion observed in fresh RBCs

(10.4%), the proportion of circulating SMEs at 5 minutes and 2 hours posttransfusion was significantly increased ($P < .0001$ and $.05$, respectively), whereas it was similar at 24 hours (Figure 5B). The decrease in 24-hour posttransfusion recovery of long-stored RBCs was mostly due to the clearance of SMEs, which had a markedly lower posttransfusion recovery (16.8%) than morphologically normal RBCs (86.8%;

Figure 4. Identification and quantification of a subpopulation of SMEs in a mouse model. (A) Posttransfusion recovery of long-stored RBCs (14 days of storage; lavender line; $n = 7$) is decreased at 2 and 24 hours after transfusion to control recipients compared with short-stored RBCs (1 day of storage; red line; $n = 7$). (B) Normalized frequency plots of projected surface area for fresh (purple line; $n = 11$) and short-stored RBCs (red line; $n = 9$) show similar patterns. (C) Long-stored RBCs (lavender line; $n = 9$) have a reduced projected surface area compared with short-stored RBCs (red line). (D) Quantification of projected surface area of front views of focused RBCs obtained by imaging flow cytometry shows a significant decrease in long-stored RBCs. (E) Representative analysis of brightfield images of long-stored RBCs shows that morphologically altered RBCs (dashed red line) have a reduced projected surface area compared with RBCs with normal morphology (blue line). Morphologically altered RBCs defined as type III echinocytes, spherocytocytes, spherostomatocytes, and spherocytes, whereas normal RBCs comprised discocytes and type I and II echinocytes. (F) SMEs in short- and long-stored RBCs accumulate during storage. Data are presented as means \pm standard errors of the mean. $***P < .001$, $****P < .0001$ by Sidak multiple comparisons test comparing, at each time point, recovery of short- vs long-stored RBCs (A), by Tukey multiple comparisons test comparing projected surface area for each condition (D), or by Student *t* test comparing proportion of SMEs in short-stored vs long-stored RBC (F). ns, not significant.



$P < .0001$; Figure 5C). Thus, ~75% of transfused long-stored RBCs cleared from the circulation were SMEs.

After transfusion, long-stored RBCs accumulate predominantly in the spleen and are mainly ingested by macrophages

Accumulation of transfused RBC was quantified in organs potentially involved in their clearance. Transfused RBC clearance

from circulation was almost linear over a 4-hour period (Figure 5D). Organ accumulation of RBCs was measured by dividing the proportion of transfused RBCs in organs by the proportion of transfused RBCs simultaneously present in circulation, a ratio expressed as EF. Long-stored RBCs accumulated in the spleen as early as 5 minutes after transfusion (EF, 2.5), with a peak at 2 hours (EF, 3.6), followed by a plateau phase up to 4 hours (EF, 3.5; Figure 5E). In the liver,

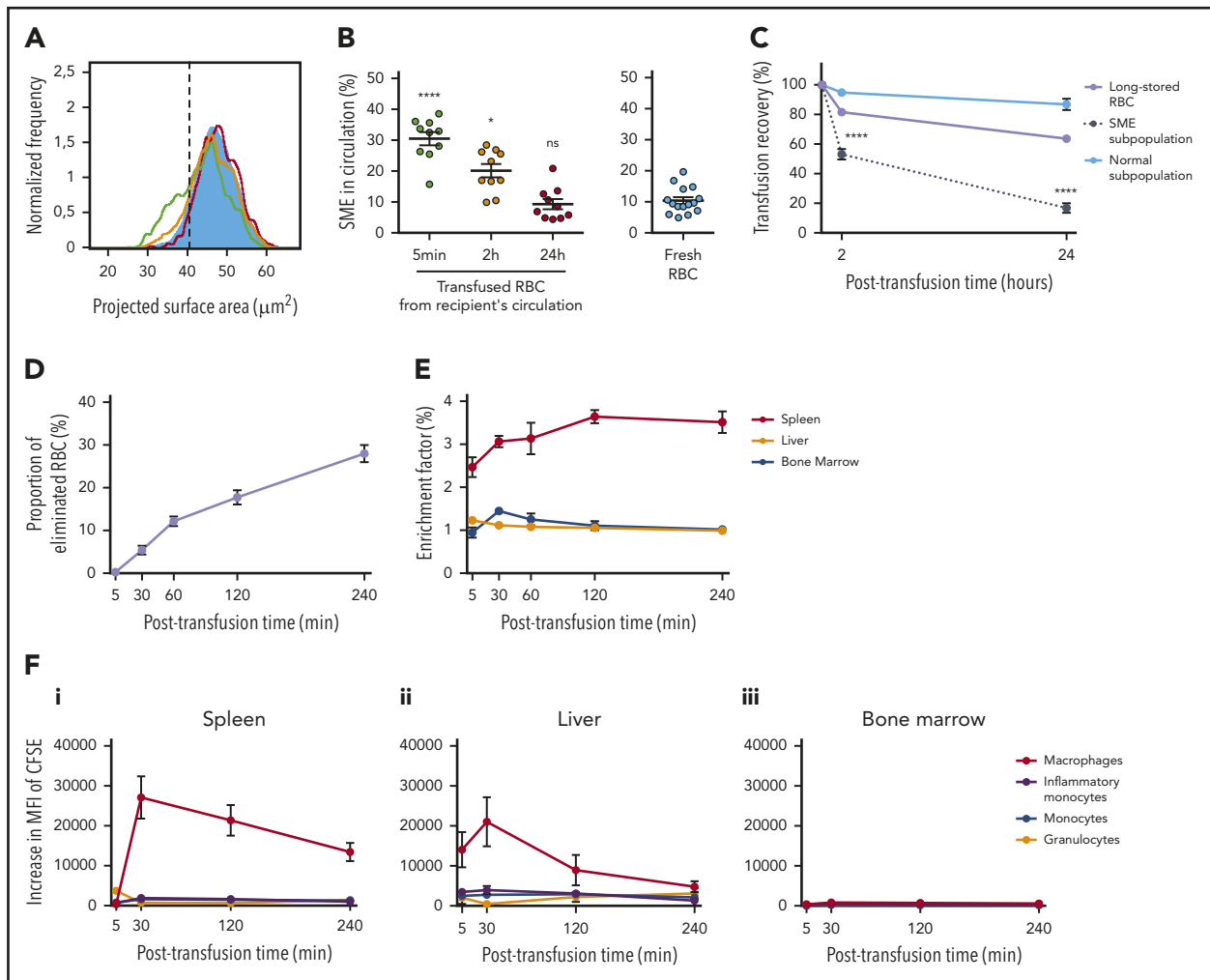


Figure 5. In the mouse model, SMEs are rapidly cleared, accumulate in the spleen, and are processed predominantly by macrophages. (A) Representative normalized frequency plot of projected surface area for long-stored mouse RBCs, as observed at 5 minutes (green line), 2 hours (yellow line), and 24 hours (red line) after transfusion to a syngeneic C57Bl/6 mouse. Control fresh RBCs from a nontransfused mouse (blue) are shown as reference. Dashed black vertical line defines the gating of SMEs. (B) Declining proportion of SMEs in circulation after transfusion ($n = 10$ mice per group). (C) Variable persistence in circulation of long-stored RBCs (lavender line) that contain the 2 complementary subpopulations of SMEs (black dotted line) and morphologically normal RBCs (light blue solid line), computed by combining flow cytometric and Imagestream data ($n = 10$ mice per group). (D) Proportion of long-stored RBCs that were cleared 5 to 240 minutes posttransfusion ($n = 8$ mice per time point). (E) EF 5 to 240 minutes posttransfusion (ratio of transfused CFSE⁺ RBCs in sliced organ/CFSE⁺ RBCs in venous blood; $n = 4$ mice per time point) in spleen (red line), liver (orange line), and bone marrow (blue line). (F) Posttransfusion erythrophagocytosis of RBCs in spleen (i), liver (ii), and bone marrow (iii), estimated by the increase in CFSE median fluorescence intensity (MFI) of macrophages (red lines), monocytes (blue lines), inflammatory monocytes (purple lines), and granulocytes (orange lines), compared with control nontransfused mice ($n = 3$ mice per time point). Data are presented as means \pm standard errors of the mean. * $P < .05$, **** $P < .0001$ by Kruskal-Wallis test compared with fresh RBC condition (B) or by Sidak multiple comparisons test comparing, at each time point, recovery of SME subpopulation vs normal subpopulation (C).

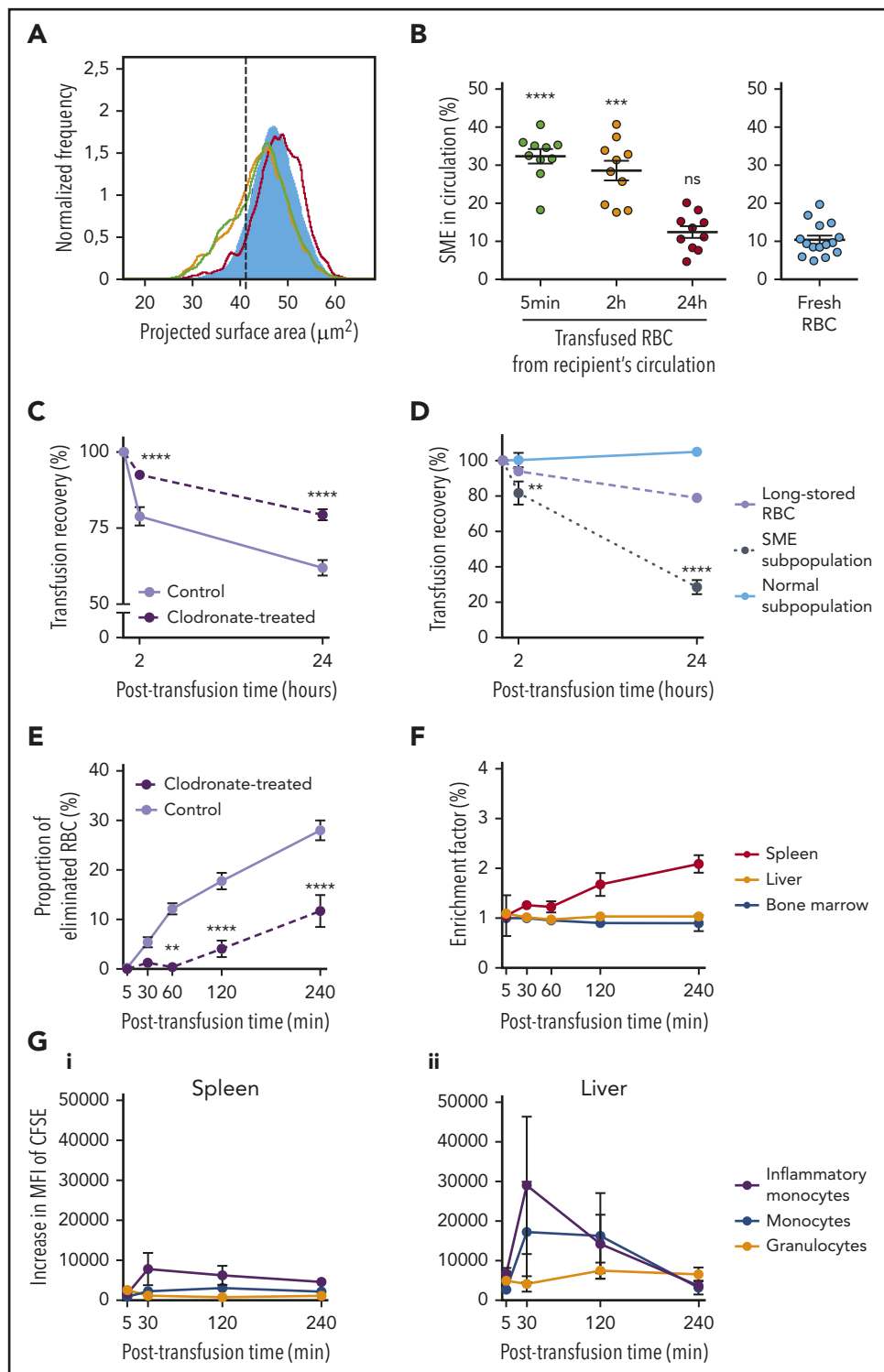
EF remained low, whereas in the bone marrow, it reached a maximum after 30 minutes (EF, 1.4). Erythrophagocytic cells in these organs were identified by quantifying their increase in CFSE fluorescence after transfusion. In the spleen, the increase in CFSE fluorescence in red pulp macrophages reached a maximum at 30 minutes (MFI, $27\,092 \pm 5299$) and remained strong up to 4 hours posttransfusion (MFI, $13\,454 \pm 2295$; Figure 5Fi). The maximum increase in CFSE fluorescence was mild in inflammatory monocytes (MFI, 1906 ± 443 at 30 minutes), monocytes (MFI, 1624 ± 334 at 30 minutes), and granulocytes (MFI, 3698 ± 687 at 5 minutes). Liver Kupffer cells also exhibited increased CFSE fluorescence, reaching a maximum at 30 minutes (MFI, $21\,023 \pm 6148$), which declined by 4 hours after transfusion (Figure 5Fii). Mild erythrophagocytosis was detected in the bone marrow (Figure 5Fiii).

SME clearance is delayed in macrophage-depleted recipients

In clodronate-treated recipients, the projected surface area of circulating RBCs was similar at 5 minutes and 2 hours after transfusion, indicating a delay in clearance of RBCs with altered morphology (Figure 6A). At 24 hours, the distribution profile of RBCs transfused into clodronate-treated recipients was similar to that of fresh RBCs. The proportion of SMEs in circulation was relatively stable over 2 hours (32.4% and 28.6% at 5 minutes and 2 hours posttransfusion, respectively) but decreased at 24 hours (12.4%; Figure 6B). The proportion of circulating SMEs at 5 minutes and 2 hours was significantly increased ($P < .0001$ and $.001$, respectively) compared with fresh RBCs. In clodronate-treated recipients, 24-hour posttransfusion recovery of long-stored RBCs was increased (79.4%) compared

Figure 6. Clearance kinetics of SMEs in clodronate-treated mice.

(A) Representative normalized frequency plots of projected surface area for long-stored mouse RBCs, as observed 5 minutes (green line), 2 hours (yellow line), and 24 hours (red line) after transfusion of a clodronate-treated mouse. Control fresh RBCs from a non-transfused mouse (blue) are shown as reference. Dashed black vertical line defines gating of SME. (B) Delayed clearance of SMEs in circulation after transfusion in clodronate-treated mice ($n = 10$ per group). (C) Posttransfusion recovery of long-stored RBCs is increased at 2 and 24 hours after transfusion to clodronate-treated recipients (dashed line; $n = 10$) compared with controls (solid line; $n = 10$). (D) Variable persistence in circulation of long-stored RBCs (lavender dashed line) that contain the 2 complementary subpopulations of SMEs (black dotted line) and morphologically normal RBCs (light blue solid line), computed by combining flow cytometric and Imagestream data after transfusion in clodronate-treated mice ($n = 10$ per group). (E) Decreased proportion of long-stored RBCs that were cleared 60 to 240 minutes posttransfusion in clodronate-treated recipients (dashed line; $n = 6$ mice per time point) compared with controls (solid line; $n = 8$ mice per time point). (F) EF (ratio of transfused CFSE⁺ RBCs in sliced organ/CFSE⁺ RBCs in venous blood) 5 to 240 minutes posttransfusion in spleen (red line), liver (orange line), and bone marrow (blue line) after transfusion in clodronate-treated mice ($n = 3$ mice per time point). (G) Posttransfusion erythrophagocytosis of RBCs in spleen (i) and liver (ii), estimated by the increase in MFI of CFSE in monocytes (blue lines), inflammatory monocytes (purple lines), and granulocytes (orange lines) in clodronate-treated recipients compared with control nontransfused mice ($n = 3$ mice per time point). Data are presented as means \pm standard errors of the mean. $^{**}P < .01$, $^{***}P < .001$, $^{****}P < .0001$ by Kruskal-Wallis test compared with fresh RBC condition (B), by Sidak multiple comparisons test comparing, at each time point, recovery (clearance) in clodronate-treated vs control recipients (C,E), and by Sidak multiple comparisons test comparing, at each time point, recovery of SME subpopulation vs normal subpopulation (D).



with controls (61.9%; $P < .0001$; Figure 6C). Similarly to control mice (Figure 4C), the SME subpopulation was preferentially cleared (24-hour posttransfusion recovery, 28.5%), whereas the proportion of morphologically normal RBCs remained stable ($P < .0001$; Figure 6D). PBS liposome-treated recipients demonstrated posttransfusion morphology, SME clearance, and recovery similar to those observed in control recipients (supplemental Figure 4).

Organ accumulation and phagocytosis of long-stored RBCs and SMEs in macrophage-depleted or splenectomized mice

In clodronate-treated recipients, early clearance of long-stored RBCs was delayed and significantly reduced at 1 ($P < .01$), 2, and 4 hours compared with controls ($P < .0001$; Figure 6E). In the spleen, EF remained <1.3 during the first hour posttransfusion and then reached 2.1 at 4 hours (Figure 6F). No

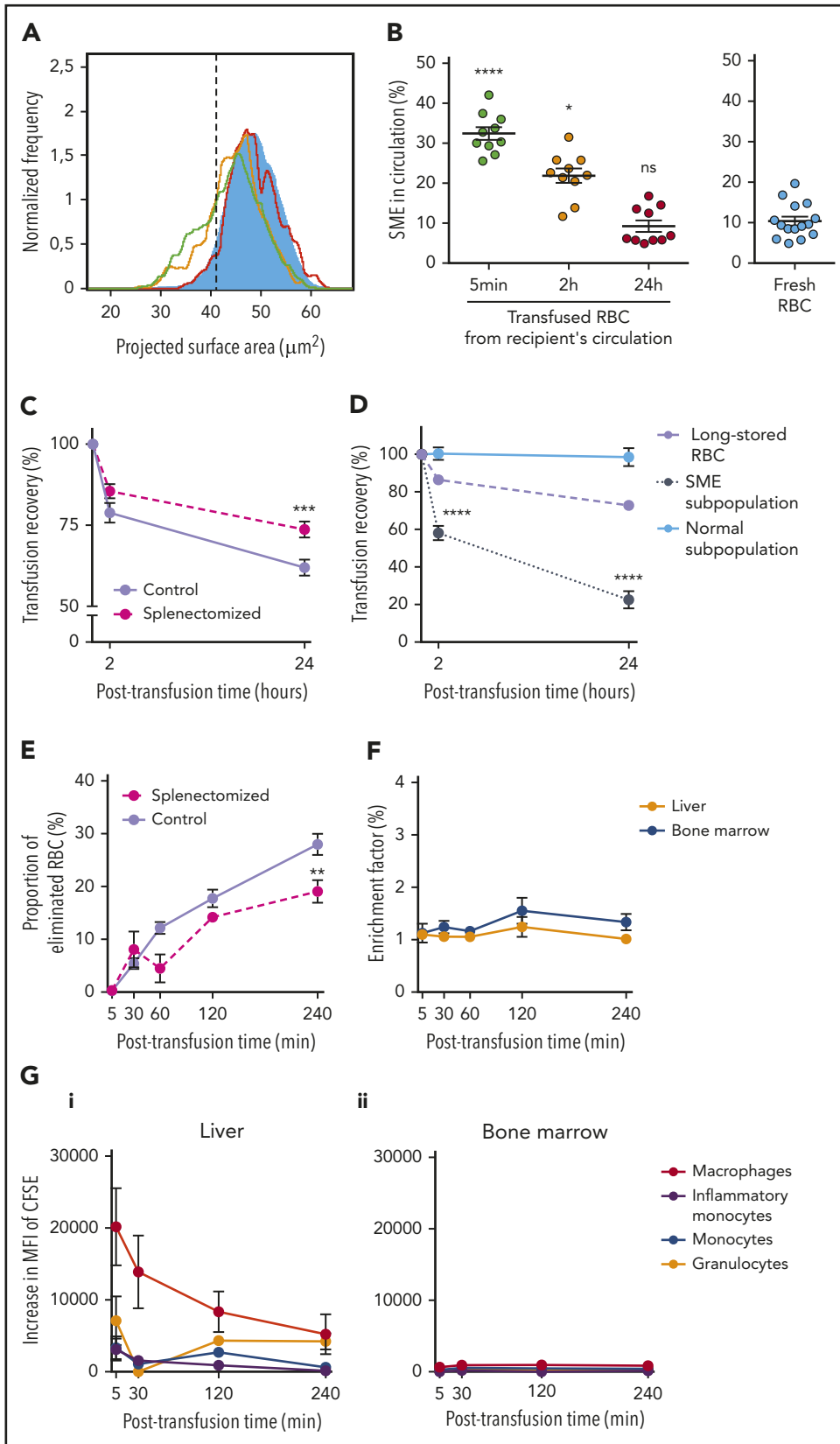


Figure 7. Clearance kinetics of SMEs in splenectomized mice. (A) Typical normalized frequency plots of projected surface area for long-stored mouse RBCs, as observed 5 minutes (green line), 2 hours (yellow line), and 24 hours (red line) after transfusion to a splenectomized mouse. Control fresh RBCs from a nontransfused mouse (blue) are shown as reference. Dashed black vertical line defines gating of SME. (B) Delayed clearance of SMEs in circulation after transfusion in splenectomized mice ($n = 10$ per group). (C) Posttransfusion recovery of long-stored RBCs is increased at 24 hours after transfusion to splenectomized recipients (dashed line; $n = 10$) compared with controls (solid line; $n = 10$). (D) Variable persistence in circulation of long-stored RBCs (lavender dashed line) that contain the 2 complementary subpopulations of SMEs (black dotted line) and morphologically normal RBCs (light blue solid line), computed by combining flow cytometric and Imagestream data, after transfusion in splenectomized mice ($n = 10$ per group). (E) Decreased proportion of long-stored RBCs that were cleared at 240 minutes posttransfusion in splenectomized recipients (dashed line; $n = 6$ mice per time point) compared with controls (solid line; $n = 8$ mice per time point). (F) EF (ratio of transfused CFSE⁺ RBCs in sliced organ/CFSE⁺ RBCs in venous blood) 5 to 240 minutes posttransfusion in liver (orange line) and bone marrow (blue line) after transfusion in splenectomized mice ($n = 3$ mice per time point). (G) Posttransfusion erythrophagocytosis of RBCs in liver (i) and bone marrow (ii), estimated by the increase in MFI of CFSE in macrophages (red lines), monocytes (blue lines), inflammatory monocytes (purple lines), and granulocytes (orange lines) in splenectomized recipients compared with control nontransfused mice ($n = 3$ mice per time point). Data are presented as means \pm standard errors of the mean. * $P < .05$, ** $P < .01$, *** $P < .001$, **** $P < .0001$ by Kruskal-Wallis test compared with fresh RBC condition (B), by Sidak multiple comparisons test comparing, at each time point, recovery (clearance) in splenectomized vs control recipients (C,E), and by Sidak multiple comparisons test comparing, at each time point, recovery of SME subpopulation vs normal subpopulation (D).

enrichment was observed in the liver or bone marrow. In the spleen of these macrophage-depleted recipients, erythrophagocytosis was observed in monocytes and inflammatory monocytes, in particular (Figure 6Gi). Similarly, in the liver,

strong erythrophagocytosis was observed in monocytes and inflammatory monocytes (Figure 6Gii). In the bone marrow, there was only a mild increase in CFSE fluorescence (data not shown).

In splenectomized mice, the surface area of transfused RBCs returned to normal at the same rate as in controls and sham-splenectomized mice (Figure 7A; supplemental Figure 4). Accordingly, SME clearance kinetics were similar in splenectomized recipients and controls (Figure 7B). Although SME clearance was not delayed or decreased in splenectomized recipients, 24-hour posttransfusion recovery of long-stored RBCs was increased (73.7%) compared with controls (61.9%; $P < .001$; Figure 7C). The main determinant of 24-hour posttransfusion recovery was the clearance of SMEs, which showed low posttransfusion recovery (22.5%) compared with normal RBCs (98.5%; $P < .0001$; Figure 7D), indicating that ~96% of the transfused long-stored RBCs cleared from circulation were SMEs. Early clearance of long-stored RBCs also decreased in splenectomized mice ($P < .01$; Figure 7E), with low retention observed in the liver and bone marrow (Figure 7F). Early erythrophagocytosis was detected in Kupffer cells and granulocytes (Figure 7Gi). Mild erythrophagocytosis was detected in the bone marrow (Figure 7Gii).

Discussion

We found that the proportion of small spherocytic RBCs that accumulated during storage correlated with posttransfusion RBC recovery in healthy human volunteers (using the gold standard of ^{51}Cr labeling) and with retention rate in human spleen perfused *ex vivo*. In a mouse RBC storage and transfusion model, we also observed the accumulation of SMEs and confirmed that they were rapidly cleared from circulation after transfusion. In both humans and mice, the spleen contributed to SME clearance from circulation. We found that SMEs progressively accumulated upon storage in commonly used preservation solutions and accounted for 20% to 25% of the entire RBC population after 6 weeks of storage.^{36,50} Only a subpopulation of RBCs was severely altered during storage, possibly corresponding to the older RBC component present in the concentrate at the beginning of storage.^{51,52} On the basis of these observations, the spherocytic shift of stored RBCs should be considered a mechanism of suboptimal transfusion recovery in humans. Thus, quantification of SMEs becomes a potentially powerful predictor of RBC storage quality and transfusion recovery. Indeed, the proportion of SMEs at the end of storage displayed wide interindividual variability, which may have contributed to the similarly wide variation in posttransfusion recovery observed previously in healthy human volunteers and patients.^{17,18,20,23}

Time-dependent decrease in circulating SMEs can result from extravascular clearance, intravascular hemolysis, or restoration of morphology (if SMEs revert to normal morphology while circulating). In macrophage-depleted mice, SMEs persisted in circulation for at least 2 hours, suggesting that simple morphological reversibility in circulation is not a major contributor to the rapid clearance observed in macrophage-intact recipients. We also showed that SME morphology was stable when suspended in fresh plasma.

Posttransfusion recovery results in macrophage-depleted mice suggest that most RBCs cleared from circulation are SMEs. The mouse *in vivo* erythrophagocytosis experiments identified splenic red pulp macrophages and hepatic Kupffer cells as important cells in this posttransfusion phagocytic process. That splenic and hepatic macrophages were the main erythrophagocytic cells in mice agrees with previous reports,^{53,54} along with the increased susceptibility of long-stored RBCs to macrophage phagocytosis

in vitro.⁵⁵ Little is known about the role of macrophages in clearance of transfused RBCs in humans, although 1 study showed increased phagocytosis of long-stored RBCs *in vitro*,⁵⁶ and another suggested that the liver and spleen are the predominant organs involved.⁵⁷ Although it cannot be excluded that some long-stored RBCs undergo intravascular destruction, converging data from mouse models strongly suggest that, as in humans,²³ the decreased posttransfusion recovery of long-stored RBCs depends predominantly on their extravascular hemolysis.

In our murine model, long-stored RBCs accumulated in the spleen, likely by mechanical filtration.⁵⁸ The simultaneous accumulation of long-stored RBCs in erythrophagocytic organs coupled with their disappearance from circulation suggests that retention of long-stored RBCs participates in their elimination. The clearance of morphologically normal RBCs, mainly observed in control recipients, could be due to proerythrophagocytic conditions induced by the accumulation of transfused RBCs in the spleen. This clearance-enhancing mechanism, called the bystander effect, has been observed in other situations, such as malaria.^{59,60} SME clearance was not affected by splenectomy in mice but was delayed by macrophage depletion, indicating that phagocytosis is indispensable and that the liver or other organs, like the kidney or lung, that were not investigated here may compensate for splenic clearance.

Type III echinocytes and spherocytocytes progressively lose membrane content through budding of microvesicles from their spicules.^{61,62} This process also occurs upon exposure of RBCs to low pH, low ATP concentrations, and high concentrations of calcium.⁶² In the context of pretransfusion refrigerated storage, this shape change is slowed by resuspension of RBCs in a large volume of solution.^{63,64} Because SMEs irreversibly lose more surface than volume upon vesiculation, they no longer display the advantageous surface/volume ratio that enables normal discocytes to readily deform and cross the narrow slits in the spleen.^{65,66} When perfused *ex vivo* with human RBCs, human spleen cleared SMEs from circulation in 2 phases. The initial phase occurred within 2 minutes of perfusion, and the second occurred between 10 and 20 minutes of perfusion. This 2-step process suggests the involvement of distinct and successive mechanisms of clearance. RBC adherence to endothelial cells could be involved in the first phase. Previous observations have suggested that this type of adherence happens rapidly,⁶⁷ whereas the timing of the second phase is compatible with biomechanical retention of SMEs upstream of narrow splenic slits. Whether the second phase relies predominantly on biomechanical retention or phagocytosis by resident macrophages remains to be determined.

The specific alterations of SMEs that induce their elimination was not definitely determined. In addition to their proadhesive properties⁶⁸ and presumed reduced deformability, SMEs may also overexpress phagocytic “eat me” surface markers, such as phosphatidylserine or clustered band 3, or conversely underexpress “don’t eat me” signals, such as CD47.⁶⁹⁻⁷¹ The fact that rejuvenation decreases both the proportion of SMEs and RBC clearance in the human spleen model also supports the adherence and biomechanical retention hypothesis, because rejuvenation reduces adherence of stored RBCs to endothelial cells and improves their filterability in a biomimetic splenic filter.⁶⁸

The extent of storage lesions varies between human blood donors and between mouse strains.^{18,20,72} One possible explanation

is that RBCs from good storers may withstand the metabolic stress of storage more robustly than RBCs from poor storers.⁷³ In addition, storage duration is a crude and potentially misleading indicator of RBC quality, because metabolic age likely differs from chronological age. In the future, more relevant markers should thus better predict RBC clearance. The 24-hour post-transfusion recovery of ⁵¹Cr-labeled RBCs in healthy volunteers is still the gold standard for US Food and Drug Administration approval of any new process for preparing and storing RBC concentrates,²⁰ but this method and other analogous methods do not recapitulate all the conditions of standard allogeneic RBC transfusion.⁷⁴ In addition, posttransfusion recovery studies using ⁵¹Cr-labeled RBCs are technically challenging, expensive, and only performed at a few centers. Furthermore, the reliability of the method was recently questioned.⁵⁷ Quantification of SMEs requires access to imaging flow cytometric technology but is otherwise a label-free, operator-independent, quantitative, reproducible, and reasonably simple method. Data presented here show that 21% of donors had high SME levels at day 42, potentially identifying them as poor storers. Similarly, 12.5% of donors exhibited low SME levels at day 42, potentially identifying them as good storers. This could be relevant for public health; for example, in France, 3.4% of RBC concentrates are transfused after storage day 35, which represents 78 000 individual transfusions per year. In addition, the proportion of such transfused RBC units may be even higher in the United States, reaching 10% to 20% by some estimates.⁷⁵ Moreover, at the median time of RBC concentrate delivery in France (16–20 days of storage), high interdonor variability is already noticeable.

If a decrease in recovery is not expected to cause serious consequences in the acute transfusion setting, it could have a major impact in chronically transfused patients, such as those with sickle cell disease, thalassemia, or low-risk myelodysplastic syndrome. For example, transfusion-related iron overload is a major cause of morbidity and mortality in these patients, and the need to provide more transfusions because some are of lower quality or recovery could have significant adverse consequences. In the future, quantifying SMEs could be a surrogate measure for transfusion recovery when assessing promising alternative storage solutions, such as AS-7⁶; new manufacturing processes, such as hypoxic storage⁷⁷; or donor-related factors that contribute to storage quality, such as those identified in REDS-III⁷⁸ and other²⁶ studies. These innovations could reduce or abrogate the transfusion of lower-quality products, with potential benefit for chronically transfused patients in whom improved transfusion recovery would be expected to decrease the degree of iron overload.

Acknowledgments

The authors thank Etablissement Français du Sang Haut de France-Normandie for providing RBC concentrates.

REFERENCES

1. Lacroix J, Hébert PC, Fergusson DA, et al; Canadian Critical Care Trials Group. Age of transfused blood in critically ill adults. *N Engl J Med*. 2015;372(15):1410-1418.
2. Dhabangi A, Ainomugisha B, Cserti-Gazdewich C, et al. Effect of transfusion of red

blood cells with longer vs shorter storage duration on elevated blood lactate levels in children with severe anemia: the TOTAL randomized clinical trial. *JAMA*. 2015;314(23):2514-2523.

3. Steiner ME, Ness PM, Assmann SF, et al. Effects of red-cell storage duration on patients

undergoing cardiac surgery. *N Engl J Med*. 2015;372(15):1419-1429.

4. Cooper DJ, McQuilten ZK, Nichol A, et al; TRANSFUSE Investigators and the Australian and New Zealand Intensive Care Society Clinical Trials Group. Age of red cells for transfusion and outcomes in critically ill adults. *N Engl J Med*. 2017;377(19):1858-1867.

This work was supported by state funding from the Agence Nationale de la Recherche under the “Investissements d’avenir” program (ANR-10-IAHU-01, ANR-11-LABX-0051, and ANR-18-IDEX-0001); the Fondation Bettencourt Schueller; the National Heart, Lung and Blood Institute, National Institutes of Health, grants R01HL133049 and HL148151; and Zimmer Biomet. A. Morel was supported by an Imagine Institute PhD scholarship. C.R., M. Colard, and M. Casimir were supported by a scholarship from the Laboratory of Excellence GR-Ex. C.R. was supported by a scholarship from the Société Française d’Hématologie.

Authorship

Contribution: C.R., A. Morel, M. Dussiot, M.M., M. Colard, A.F.-M., A. Martinez, C.C., B.H., M. Casimir, G.V., M. Dépond, S.G., E.A.H., and P.A. performed experiments; C.R., A. Morel, M. Dussiot, M.M., M. Colard, A.F.-M., A. Martinez, C.C., B.H., M. Casimir, G.V., M. Dépond, C.L.V.K., Y.C., S.G., P.R., S.L.S., P.A.N., O.H., E.A.H., P.A.B., and P.A. analyzed the data; S.D., F.P., and A.S. provided human spleens; C.R., A. Morel, M. Dussiot, P.A.N., S.L.S., O.H., E.A.H., P.A.B., and P.A. designed the research; C.R., A. Morel, M. Dussiot, P.A.B., and P.A. wrote the manuscript; S.L.S. and E.A.H. edited the manuscript; and all authors read and approved the manuscript.

Conflict-of-interest disclosure: P.A.B. and P.A. are funded in part by Zimmer Biomet. The remaining authors declare no competing financial interests.

ORCID profiles: C.R., 0000-0003-0194-7696; M. Dussiot, 0000-0002-6804-1621; M.M., 0000-0002-4094-022X; M. Colard, 0000-0001-8247-0505; B.H., 0000-0003-4916-4121; S.D., 0000-0002-3335-4388; F.P., 0000-0002-7193-2628; A.S., 0000-0002-7436-5999; C.L.V.K., 0000-0002-3251-1310; Y.C., 0000-0001-5196-4254; S.G., 0000-0002-2567-8593; P.R., 0000-0001-9131-3341; S.L.S., 0000-0002-8528-4561; P.A.N., 0000-0001-7203-9754; O.H., 0000-0003-2574-3874; E.A.H., 0000-0002-2367-9509; P.A.B., 0000-0003-4010-929X; P.A., 0000-0002-5562-7586.

Correspondence: Pascal Amireault, Institut National de la Transfusion Sanguine, 6 Rue Alexandre Cabanel, F-75015 Paris, France; e-mail: pascal.amireault@inserm.fr; and Pierre A. Buffet, Institut National de la Transfusion Sanguine, 6 Rue Alexandre Cabanel, F-75015 Paris, France; e-mail: pabuffet@gmail.com.

Footnotes

Submitted 5 August 2020; accepted 16 January 2021; prepublished online on *Blood* First Edition 3 March 2021. DOI 10.1182/blood.2020008563.

*C.R., A. Morel, and M. Dussiot are joint first authors.

†P.A.B. and P.A. are joint senior authors.

For original data, please contact pascal.amireault@inserm.fr.

The online version of this article contains a data supplement.

There is a *Blood* Commentary on this article in this issue.

The publication costs of this article were defrayed in part by page charge payment. Therefore, and solely to indicate this fact, this article is hereby marked “advertisement” in accordance with 18 USC section 1734.

5. Heddle NM, Cook RJ, Arnold DM, et al. Effect of short-term vs. long-term blood storage on mortality after transfusion. *N Engl J Med*. 2016;375(20):1937-1945.
6. McQuilten ZK, French CJ, Nichol A, Higgins A, Cooper DJ. Effect of age of red cells for transfusion on patient outcomes: a systematic review and meta-analysis [published correction appears in *Transfus Med Rev*. 2020;34(2):138-139]. *Transfus Med Rev*. 2018;32(2):77-88.
7. Chai-Adisaksopha C, Alexander PE, Guyatt G, et al. Mortality outcomes in patients transfused with fresher versus older red blood cells: a meta-analysis. *Vox Sang*. 2017;112(3):268-278.
8. Cook RJ, Heddle NM, Lee K-A, et al. Red blood cell storage and in-hospital mortality: a secondary analysis of the INFORM randomized controlled trial. *Lancet Haematol*. 2017;4(11):e544-e552.
9. Cartotto R, Taylor SL, Holmes JH IV, et al. The effects of storage age of blood in massively transfused burn patients: a secondary analysis of the randomized transfusion requirement in burn care evaluation study. *Crit Care Med*. 2018;46(12):e1097-e1104.
10. Jones AR, Patel RP, Marques MB, et al; PROPPR Study Group. Older blood is associated with increased mortality and adverse events in massively transfused trauma patients: secondary analysis of the PROPPR trial. *Ann Emerg Med*. 2019;73(6):650-661.
11. Högman CF, Meryman HT. Storage parameters affecting red blood cell survival and function after transfusion. *Transfus Med Rev*. 1999;13(4):275-296.
12. Högman CF, Meryman HT. Red blood cells intended for transfusion: quality criteria revisited. *Transfusion*. 2006;46(1):137-142.
13. Greenwalt TJ. The how and why of exocytic vesicles. *Transfusion*. 2006;46(1):143-152.
14. D'Alessandro A, Kriebardis AG, Rinalducci S, et al. An update on red blood cell storage lesions, as gleaned through biochemistry and omics technologies. *Transfusion*. 2015;55(1):205-219.
15. Yoshida T, Prudent M, D'Alessandro A. Red blood cell storage lesion: causes and potential clinical consequences. *Blood Transfus*. 2019;17(1):27-52.
16. Hess JR, Greenwalt TG. Storage of red blood cells: new approaches. *Transfus Med Rev*. 2002;16(4):283-295.
17. Luten M, Roerdinkholder-Stoelwinder B, Schaap NPM, de Grip WJ, Bos HJ, Bosman GJ. Survival of red blood cells after transfusion: a comparison between red cells concentrates of different storage periods. *Transfusion*. 2008;48(7):1478-1485.
18. Dem RJ, Gwinn RP, Wiorkowski JJ. Studies on the preservation of human blood. I. Variability in erythrocyte storage characteristics among healthy donors. *J Lab Clin Med*. 1966;67(6):955-965.
19. Hess JR, Sparrow RL, van der Meer PF, Acker JP, Cardigan RA, Devine DV. Red blood cell hemolysis during blood bank storage: using national quality management data to answer basic scientific questions. *Transfusion*. 2009;49(12):2599-2603.
20. Dumont LJ, AuBuchon JP. Evaluation of proposed FDA criteria for the evaluation of radiolabeled red cell recovery trials. *Transfusion*. 2008;48(6):1053-1060.
21. Prudent M, Tissot J-D, Lion N. In vitro assays and clinical trials in red blood cell aging: lost in translation. *Transfus Apheresis Sci*. 2015;52(3):270-276.
22. Baryn M, Rappaz B, Jaferzadeh K, et al. Red blood cells ageing markers: a multi-parametric analysis. *Blood Transfus*. 2017;15(3):239-248.
23. Rapido F, Brittenham GM, Bandyopadhyay S, et al. Prolonged red cell storage before transfusion increases extravascular hemolysis. *J Clin Invest*. 2017;127(1):375-382.
24. Rydén J, Clements M, Hellström-Lindberg E, Höglund P, Edgren G. A longer duration of red blood cell storage is associated with a lower hemoglobin increase after blood transfusion: a cohort study. *Transfusion*. 2019;59(6):1945-1952.
25. Hunsicker O, Hessler K, Krannich A, et al. Duration of storage influences the hemoglobin rising effect of red blood cells in patients undergoing major abdominal surgery. *Transfusion*. 2018;58(8):1870-1880.
26. Roubinian NH, Plimier C, Woo JP, et al. Effect of donor, component, and recipient characteristics on hemoglobin increments following red blood cell transfusion. *Blood*. 2019;134(13):1003-1013.
27. Hess JR; Biomedical Excellence for Safer Transfusion (BEST) Collaborative. Scientific problems in the regulation of red blood cell products. *Transfusion*. 2012;52(8):1827-1835.
28. Ashby W. The determination of the length of life of transfused blood corpuscles in man. *J Exp Med*. 1919;29(3):267-281.
29. Haradin AR, Weed RI, Reed CF. Changes in physical properties of stored erythrocytes relationship to survival in vivo. *Transfusion*. 1969;9(5):229-237.
30. Högman CF, de Verdier CH, Ericson A, Hedlund K, Sandhagen B. Studies on the mechanism of human red cell loss of viability during storage at +4 degrees C in vitro. I. Cell shape and total adenylate concentration as determinant factors for posttransfusion survival. *Vox Sang*. 1985;48(5):257-268.
31. Szymanski IO, Valeri CR, McCallum LE, Emerson CP, Rosenfield RE. Automated differential agglutination technic to measure red cell survival. I. Methodology. *Transfusion*. 1968;8(2):65-73.
32. Gabrio BW, Donohue DM, Finch CA. Erythrocyte preservation. V. Relationship between chemical changes and viability of stored blood treated with adenosine. *J Clin Invest*. 1955;34(10):1509-1512.
33. Valeri CR, Pivacek LE, Palter M, et al. A clinical experience with ADSOL preserved erythrocytes. *Surg Gynecol Obstet*. 1988;166(1):33-46.
34. Heaton WA, Holme S, Smith K, et al. Effects of 3-5 log10 pre-storage leucocyte depletion on red cell storage and metabolism. *Br J Haematol*. 1994;87(2):363-368.
35. Reid TJ, Babcock JG, Derse-Anthony CP, Hill HR, Lippert LE, Hess JR. The viability of autologous human red cells stored in additive solution 5 and exposed to 25 degrees C for 24 hours. *Transfusion*. 1999;39(9):991-997.
36. Roussel C, Dussiot M, Marin M, et al. Spherocytic shift of red blood cells during storage provides a quantitative whole cell-based marker of the storage lesion. *Transfusion*. 2017;57(4):1007-1018.
37. Lutz HU, Liu SC, Palek J. Release of spectrin-free vesicles from human erythrocytes during ATP depletion. I. Characterization of spectrin-free vesicles. *J Cell Biol*. 1977;73(3):548-560.
38. Greenwalt TJ, Zehner Sostok C, Dumaswala UJ. Studies in red blood cell preservation. 2. Comparison of vesicle formation, morphology, and membrane lipids during storage in AS-1 and CPDA-1. *Vox Sang*. 1990;58(2):90-93.
39. Kriebardis AG, Antonelou MH, Stamoulis KE, Economou-Petersen E, Margaritis LH, Papassideri IS. RBC-derived vesicles during storage: ultrastructure, protein composition, oxidation, and signaling components. *Transfusion*. 2008;48(9):1943-1953.
40. Safeukui I, Buffet PA, Deplaine G, et al. Quantitative assessment of sensing and sequestration of spherocytic erythrocytes by the human spleen. *Blood*. 2012;120(2):424-430.
41. Moroff G, Sohmer PR, Button LN. Proposed standardization of methods for determining the 24-hour survival of stored red cells. *Transfusion*. 1984;24(2):109-114.
42. Bitan ZC, Zhou A, McMahon DJ, et al. Donor Iron Deficiency Study (DIDS): protocol of a study to test whether iron deficiency in blood donors affects red blood cell recovery after transfusion. *Blood Transfus*. 2019;17(4):274-280.
43. Buffet PA, Milon G, Brousse V, et al. Ex vivo perfusion of human spleens maintains clearing and processing functions. *Blood*. 2006;107(9):3745-3752.
44. Fischer D, Büssow J, Meybohm P, Zacharowski K, Jennewein C. Novel method to leukoreduce murine blood for transfusion: how to reduce animal usage. *Transfusion*. 2016;56(1):146-152.
45. Bessis M. Red cell shapes. An illustrated classification and its rationale. *Nouv Rev Fr Hematol*. 1972;12(6):721-745.
46. Berezina TL, Zaets SB, Morgan C, et al. Influence of storage on red blood cell rheological properties. *J Surg Res*. 2002;102(1):6-12.
47. D'Alessandro A, D'Amici GM, Vaglio S, Zolla L. Time-course investigation of SAGM-stored leukocyte-filtered red blood cell concentrates: from metabolism to proteomics. *Haematologica*. 2012;97(1):107-115.
48. Blasi B, D'Alessandro A, Ramundo N, Zolla L. Red blood cell storage and cell morphology. *Transfus Med*. 2012;22(2):90-96.
49. D'Alessandro A, Gray AD, Szczepiorkowski ZM, Hansen K, Herschel LH, Dumont LJ. Red blood cell metabolic responses to refrigerated storage, rejuvenation, and frozen storage. *Transfusion*. 2017;57(4):1019-1030.

50. Roussel C, Monnier S, Dussiot M, et al. Fluorescence exclusion: a simple method to assess projected surface, volume and morphology of red blood cells stored in blood bank. *Front Med (Lausanne)*. 2018;5:164.
51. Tuo W-W, Wang D, Liang W-J, Huang Y-X. How cell number and cellular properties of blood-banked red blood cells of different cell ages decline during storage. *PLoS One*. 2014; 9(8):e105692.
52. Mykhailova O, Olafson C, Turner TR, D'Alessandro A, Acker JP. Donor-dependent aging of young and old red blood cell subpopulations: metabolic and functional heterogeneity. *Transfusion*. 2020;60(11): 2633-2646.
53. Hod EA, Zhang N, Sokol SA, et al. Transfusion of red blood cells after prolonged storage produces harmful effects that are mediated by iron and inflammation. *Blood*. 2010;115(21): 4284-4292.
54. Hudson KE, de Wolski K, Kapp LM, Richards AL, Schniederjan MJ, Zimring JC. Antibodies to senescent antigen and C3 are not required for normal red blood cell lifespan in a murine model. *Front Immunol*. 2017;8:1425.
55. Wojczyk BS, Kim N, Bandyopadhyay S, et al. Macrophages clear refrigerator storage-damaged red blood cells and subsequently secrete cytokines in vivo, but not in vitro, in a murine model. *Transfusion*. 2014;54(12): 3186-3197.
56. Veale MF, Healey G, Sparrow RL. Longer storage of red blood cells is associated with increased in vitro erythrophagocytosis. *Vox Sang*. 2014;106(3):219-226.
57. Francis RO, Mahajan S, Rapido F, et al. Reexamination of the chromium-51-labeled posttransfusion red blood cell recovery method. *Transfusion*. 2019;59(7):2264-2275.
58. MacDonald IC, Schmidt EE, Groom AC. The high splenic hematocrit: a rheological consequence of red cell flow through the reticular meshwork. *Microvasc Res*. 1991;42(1):60-76.
59. Douglas NM, Anstey NM, Buffet PA, et al. The anaemia of *Plasmodium vivax* malaria. *Malar J*. 2012;11:135.
60. White NJ. Anaemia and malaria. *Malar J*. 2018;17(1):371.
61. Laczkó J, Szabolcs M, Jóna I. Vesicle release from erythrocytes during storage and failure of rejuvenation to restore cell morphology. *Haematologia (Budap)*. 1985;18(4):233-248.
62. Hess JR. Red cell changes during storage. *Transfus Apheresis Sci*. 2010;43(1):51-59.
63. Meryman HT, Hornblower M, Syring R, Mesbah-Karimi N. Extending the storage of red cells at 4 degrees C. *Transfus Sci*. 1994; 15(2):105-115.
64. Meryman HT. Quarantine of red blood cells by long-term storage in the liquid phase. *Transfus Clin Biol*. 1994;1(3):188-191.
65. Perrotta S, Gallagher PG, Mohandas N. Hereditary spherocytosis. *Lancet*. 2008; 372(9647):1411-1426.
66. Waugh RE, Sarelius IH. Effects of lost surface area on red blood cells and red blood cell survival in mice. *Am J Physiol*. 1996;271(6 Pt 1):C1847-C1852.
67. Safeukui I, Correas J-M, Brousse V, et al. Retention of *Plasmodium falciparum* ring-infected erythrocytes in the slow, open microcirculation of the human spleen. *Blood*. 2008;112(6):2520-2528.
68. Marin M, Roussel C, Dussiot M, et al. Metabolic rejuvenation upgrades circulatory functions of red blood cells stored under blood bank conditions [published online ahead of print 31 December 2020]. *Transfusion*. doi:10.1111/trf.16245.
69. Verhoeven AJ, Hilarius PM, Dekkers DWC, Lagerberg JWM, de Korte D. Prolonged storage of red blood cells affects aminophospholipid translocase activity. *Vox Sang*. 2006;91(3):244-251.
70. Azouzi S, Romana M, Arashiki N, et al. Band 3 phosphorylation induces irreversible alterations of stored red blood cells. *Am J Hematol*. 2018;93(5):E110-E112.
71. Anniss AM, Sparrow RL. Expression of CD47 (integrin-associated protein) decreases on red blood cells during storage. *Transfus Apheresis Sci*. 2002;27(3):233-238.
72. Zimring JC, Smith N, Stowell SR, et al. Strain-specific red blood cell storage, metabolism, and eicosanoid generation in a mouse model. *Transfusion*. 2014;54(1):137-148.
73. D'Alessandro A, Zimring JC, Busch M. Chronological storage age and metabolic age of stored red blood cells: are they the same? *Transfusion*. 2019;59(5):1620-1623.
74. Roussel C, Buffet PA, Amireault P. Measuring post-transfusion recovery and survival of red blood cells: strengths and weaknesses of chromium-51 labeling and alternative methods. *Front Med (Lausanne)*. 2018;5:130.
75. Glynn SA, Klein HG, Ness PM. The red blood cell storage lesion: the end of the beginning. *Transfusion*. 2016;56(6):1462-1468.
76. Cancelas JA, Dumont LJ, Maes LA, et al. Additive solution-7 reduces the red blood cell cold storage lesion. *Transfusion*. 2015;55(3): 491-498.
77. Dumont LJ, Yoshida T, AuBuchon JP. Anaerobic storage of red blood cells in a novel additive solution improves in vivo recovery. *Transfusion*. 2009;49(3): 458-464.
78. Lanteri MC, Kaniyas T, Keating S, et al; NHLBI Recipient Epidemiology Donor Evaluation Study (REDS)-III Program. Intradonor reproducibility and changes in hemolytic variables during red blood cell storage: results of recall phase of the REDS-III RBC-Omics study. *Transfusion*. 2019;59(1): 79-88.